ON THE EFFECTS OF CARRIER FREQUENCY OFFSET ON CYCLIC PREFIX BASED OFDM AND FILTER BANK BASED MULTICARRIER SYSTEMS

Qing Bai and Josef A. Nossek

Institute for Circuit Theory and Signal Processing
Technische Universität München, Munich, Germany
Email: {bai.qing, nossek}@nws.ei.tum.de

ABSTRACT

Being sensitive to carrier frequency offset (CFO) is known to be one of the main drawbacks of multicarrier systems. In this paper, the effects of CFO on a filter bank based multicarrier system (FBMC) in a multipath fading channel are discussed, where an ideal root-raised cosine (RRC) filter with roll-off factor 1 is used as the prototype filter which enables analytical derivations of the interference caused by the CFO. Based on these results, an approximation on the SNR degradation with very small CFO is also given. Numerical experiments as well as Monte Carlo simulations are done to verify the analysis and the accuracy of the approximation in FBMC systems. A comparison with the SNR degradations in cyclic prefix based orthogonal frequency division multiplexing (CP-OFDM) systems has indicated an advantage of FBMC systems as being more robust to frequency misalignments.

1. INTRODUCTION

Despite their well-known advantages such as the ability to support high data rates through frequency selective channels, one of the main drawbacks of multicarrier systems is their sensitivity to synchronization errors in the frequency domain [1]. The CFO is mainly caused by Doppler shift due to mobility and the inherent difference between the oscillators at the transmitter and receiver. It typically destroys the orthogonality between adjacent subcarriers and results in an attenuation of the desired signal and the introduction of intercarrier interference (ICI) and possible intersymbol interference (ISI).

OFDM with cyclic prefix (CP) is by far the most popular special case of multicarrier systems and has been adopted in many current applications and standards. It has an efficient implementation by using the fast Fourier Transform (FFT) and requires very simple equalization as long as the CP exceeds the delay spread of the channel impulse response. However, the CP is purely redundant in terms of information and considerably reduces the bandwidth efficiency. On the other hand, FBMC systems provide a better spectral shaping of subcarriers than OFDM systems by careful designs of the prototype filter. In FBMC systems, each subcarrier is designed to overlap only with its immediate neighboring subcarriers, which not only simplifies equalization in the absence of CP, but also improves the robustness of the system against a potential CFO. By employing offset quadrature amplitude modulation (OQAM), the full capacity of the transmission bandwidth can be achieved in FBMC systems.

The effects of CFO on single carrier systems and CP-OFDM systems have been extensively studied in the literature, *e.g.*, [2][3][4]. There has been several recent works on this aspect in FBMC systems, *e.g.*, [5][6], which are in general based on studies and simulations of practical systems. In this work, by employing an ideal RRC filter as the prototype filter in FBMC systems, we provide exact analytical results that are comparable to the work done with CP-OFDM systems. The performance metric employed to compare the two systems is the *SNR degradation* $D(\varepsilon)$ defined as

$$D(\varepsilon) = \text{SINR}(0)|_{\text{dB}} - \text{SINR}(\varepsilon)|_{\text{dB}}, \tag{1}$$

where $\varepsilon \triangleq \frac{f_{\text{T}} - f_{\text{R}}}{\Delta f}$ is the CFO between the transmitter frequency f_{T} and the receiver frequency f_{R} normalized with the subcarrier spacing Δf, and $\text{SINR}(\varepsilon)$ denotes the signal-to-interference-plus-noise ratio as a function of ε. In addition, we assume that there is also a phase offset ϕ between the transmitter and the receiver, and the system is perfectly synchronized in the time domain. Further more, we restrict ε to be in the range $(-0.5, 0.5]$, as the integer part of the normalized frequency offset does not affect the SINR.

2. TWO IMPLEMENTATIONS OF MULTICARRIER MODULATION

The equivalent baseband models of the CP-OFDM system and the FBMC system are shown in Fig. 1, where the receive signal is corrupted by the carrier frequency and phase offset at the front end of the receiver. In FBMC systems, the real and imaginary parts of the modulated data symbols of rate $\frac{1}{T}$ are first separated by the "C2R" module and multiplied with $\theta_{n,l} = j^{n+l}$ which results in an actual transmission rate of $\frac{2}{T}$, and then modulated by the synthesis filter bank (SFB) which uniformly shifts the prototype filter $p(t)$ in the frequency to cover the whole signal bandwidth, and outputs the sum of

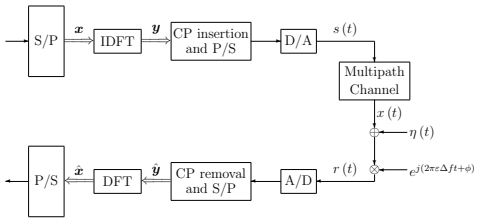

(a) CP-OFDM system model

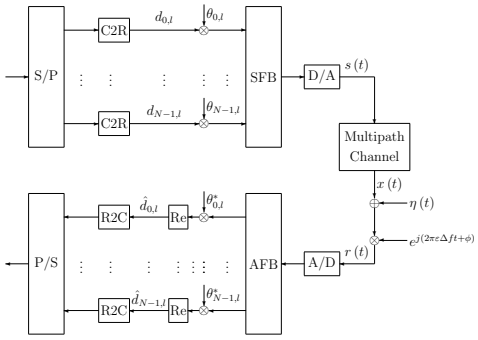

(b) FBMC system model

Fig. 1. Equivalent baseband system models

signals associated with all subcarriers. At the receiver side, the received signal is passed through the analysis filter bank (AFB) where it is demodulated and filtered by the matched filter of $p(t)$, and the complex modulated symbols are recovered from the detected OQAM symbols. Both SFB and AFB can be implemented efficiently with an IFFT/FFT module followed by polyphase filtering, yet the complexity of FBMC systems is typically higher than CP-OFDM systems.

In the next we consider the RRC filter with roll-off factor 1 as the prototype filter $p(t)$ which has the frequency response

$$H_{\mathrm{RRC}}(f) = \begin{cases} \sqrt{T}\cos\frac{\pi T f}{2}, & 0 \le |f| \le \frac{1}{T}, \\ 0, & |f| > \frac{1}{T}, \end{cases}$$

where T is the symbol duration. The better spectral shaping of subcarriers of such a system as compared with the CP-OFDM system is illustrated in Fig. 2.

3. REVIEW ON THE EFFECTS OF CFO ON CP-OFDM SYSTEM

With a CP longer than the channel impulse response, the data transmission in CP-OFDM systems is independent from block to block, where each block contains N modulated data symbols which is usually referred to as an OFDM symbol. Let the kth OFDM symbol be $\boldsymbol{x}[k] \in \mathbb{C}^N$. The transmitted vector before the insertion of the CP is $\boldsymbol{y}[k] = \boldsymbol{F}^{\mathrm{H}}\boldsymbol{x}[k]$, where $\boldsymbol{F} \in \mathbb{C}^{N\times N}$ is the unitary DFT matrix. The effect of CFO can be formulated into a diagonal matrix [3] as

$$\boldsymbol{C}[k] = e^{j\phi}\cdot e^{j2\pi\varepsilon k(1+\frac{N_{\mathrm{P}}}{N})}\cdot \mathrm{diag}\left\{1, e^{j2\pi\frac{\varepsilon}{N}}, \cdots, e^{j2\pi\frac{\varepsilon(N-1)}{N}}\right\},$$

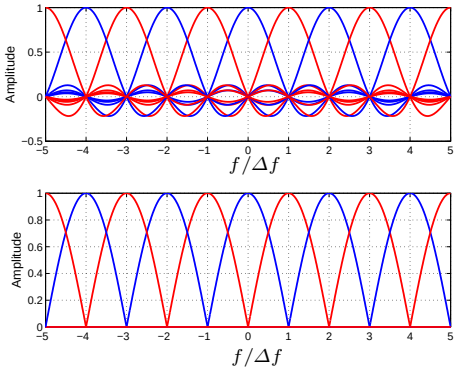

Fig. 2. OFDM and FBMC subcarriers

where N_{P} denotes the length of CP, and the received signal after the removal of the CP is given by

$$\hat{\boldsymbol{y}}[k] = \boldsymbol{C}[k]\boldsymbol{H}[k]\boldsymbol{y}[k] + \boldsymbol{\eta}[k], \tag{2}$$

where $\boldsymbol{H}[k] \in \mathbb{C}^{N\times N}$ contains the channel impulse response of the block and is a circulant matrix due to the CP, and $\boldsymbol{\eta}[k]$ represents the additive white Gaussian noise at the receiver.

If no compensation of the CFO is considered before the DFT at the receiver, the received OFDM symbol in the frequency domain is given by

$$\begin{aligned} \hat{\boldsymbol{x}}[k] &= \boldsymbol{F}\boldsymbol{C}[k]\boldsymbol{H}[k]\boldsymbol{F}^{\mathrm{H}}\boldsymbol{x}[k] + \boldsymbol{F}\boldsymbol{\eta}[k] \\ &= \boldsymbol{U}[k]\boldsymbol{\Lambda}[k]\boldsymbol{x}[k] + \boldsymbol{F}\boldsymbol{\eta}[k], \end{aligned} \tag{3}$$

where $\boldsymbol{\Lambda}[k] \in \mathbb{C}^{N\times N}$ is a diagonal matrix containing the DFT of the channel impulse response and $\boldsymbol{U}[k] \in \mathbb{C}^{N\times N}$ is a circulant matrix defined by

$$\boldsymbol{U}[k] = e^{j\phi}e^{j2\pi\varepsilon k(1+\frac{N_{\mathrm{P}}}{N})} \cdot \begin{bmatrix} \nu_N(\varepsilon,0) & \nu_N(\varepsilon,N-1) & \cdots & \nu_N(\varepsilon,1) \\ \nu_N(\varepsilon,1) & \nu_N(\varepsilon,0) & \cdots & \nu_N(\varepsilon,2) \\ \vdots & \vdots & \ddots & \vdots \\ \nu_N(\varepsilon,N-1) & \nu_N(\varepsilon,N-2) & \cdots & \nu_N(\varepsilon,0) \end{bmatrix}, \tag{4}$$

where $\nu_N(\varepsilon,n) = \frac{1}{N}\frac{\sin(\pi(\varepsilon-n))}{\sin\frac{\pi(\varepsilon-n)}{N}}e^{j\pi\frac{(\varepsilon-n)(N-1)}{N}}$.

From (3) and (4) it can be seen that the symbol detected on subcarrier n is scaled in magnitude by $|\nu_N(\varepsilon,0)|$, rotated by $e^{j(\phi+\angle H_n)}e^{j2\pi\varepsilon k(1+\frac{N_{\mathrm{P}}}{N})}e^{j\pi\frac{\varepsilon(N-1)}{N}}$, and further interfered by received symbols on the other subcarriers scaled by the corresponding off-diagonal elements of $\boldsymbol{U}[k]\boldsymbol{\Lambda}[k]$. For coherent demodulation at the receiver, the phase rotation should be estimated and we assume that it is perfectly compensated. Moreover, we assume that the data symbols transmitted on each subcarrier are independent from each other, and that the power is uniformly allocated to all subcarriers. The SINR on subcarrier n can then be expressed as

$$\mathrm{SINR}_n(\varepsilon) = \frac{|\nu_N(\varepsilon,0)|^2|H_n|^2P_{\mathrm{S}}}{\sum\limits_{\substack{n'=0\\n'\neq n}}^{N-1}|\nu_N(\varepsilon,n'-n)|^2|H_{n'}|^2P_{\mathrm{S}} + \mathrm{E}[|\boldsymbol{F}\boldsymbol{\eta}|^2]},$$

where P_{S} is the transmit power for each data symbol, and $\mathrm{E}[|\boldsymbol{F}\boldsymbol{\eta}|^2]$ equals the noise power on one subcarrier as the DFT operation does not change the power.

For flat fading channels and for small ε such that $|\varepsilon| \ll \frac{1}{\pi}$, [3] has provided an approximation of $D(\varepsilon)$ as

$$D(\varepsilon) \approx \frac{10}{\ln 10}\left(1-\frac{1}{N^2}\right)\frac{\mathrm{SNR}+1}{3}\pi^2\varepsilon^2, \tag{5}$$

where SNR stands for $\mathrm{SINR}(0)$ for simplicity.

4. EFFECTS OF CFO ON FBMC SYSTEMS

As introduced in Sec. 2, with OQAM modulation, the transmit signal $s(t)$ in an FBMC system can be written as

$$\begin{aligned} s(t) &= \sum_{n'=0}^{N-1}\sum_{l'=-\infty}^{+\infty} d_{n',l'}\theta_{n',l'}p(t-l'\frac{T}{2})e^{j2\pi\frac{n'}{T}(t-l'\frac{T}{2})} \\ &= \sum_{n'=0}^{N-1}\sum_{l'=-\infty}^{+\infty} d_{n',l'}\lambda_{n',l'}p(t-l'\frac{T}{2})e^{j2\pi\frac{n'}{T}t}, \end{aligned} \tag{6}$$

where n' is the subcarrier index, l' is the symbol index in the transmit data sequence, $\lambda_{n',l'} = \theta_{n',l'}e^{-j\pi n'l'}$, and $d_{n',l'} \in \mathbb{R}$ is alternatively the real or imaginary part of the QAM symbol loaded subcarrier n'. Note that the subcarrier spacing in such a system equals $1/T$.

The received signal $r(t)$ as indicated in Fig. 1 is given by

$$r(t) = (h(t) \otimes s(t) + \eta(t)) \cdot e^{j(2\pi\frac{\varepsilon}{T}t+\phi)}, \tag{7}$$

and then passed through the AFB and sampled at each output at rate $\frac{2}{T}$. The detected symbol on subcarrier n at symbol index l, namely $\hat{d}_{n,l}$, is therefore expressed as

$$\begin{aligned} \hat{d}_{n,l} &= \Re\left\{\lambda_{n,l}^* \cdot e^{j\phi}\left(x(t)\cdot e^{j2\pi\frac{\varepsilon-n}{T}t}\right)\otimes\tilde{p}(t)\Big|_{t=l\cdot\frac{T}{2}}\right\} + \\ &\quad \Re\left\{\lambda_{n,l}^* \cdot e^{j\phi}\left(\eta(t)\cdot e^{j2\pi\frac{\varepsilon-n}{T}t}\right)\otimes\tilde{p}(t)\Big|_{t=l\cdot\frac{T}{2}}\right\} \\ &\triangleq R_1 + R_2, \end{aligned}$$

where $x(t) = h(t) \otimes s(t)$, $\tilde{p}(t)$ is the matched filter of $p(t)$ which is known to be $p(t)$ itself, and we denote the two summation terms as R_1 and R_2. Note that $\otimes$ denotes the convolution operation and * denotes the complex conjugate operation.

Let the frequency response of $x(t)$ be $X(f)$. Applying the convolution theorem, we have $X(f) = H(f)S(f)$ where $H(f)$ and $S(f)$ are the frequency response of the multipath channel and the transmit signal, as well as

$$\begin{aligned} &\left(x(t)\cdot e^{j2\pi\frac{\varepsilon-n}{T}t}\right)\otimes\tilde{p}(t)\Big|_{t=l\cdot\frac{T}{2}} \\ &= \int_{-\infty}^{+\infty} e^{j2\pi l\frac{T}{2}f}X(f-\frac{\varepsilon-n}{T})H_{\mathrm{RRC}}(f)\mathrm{d}f. \end{aligned} \tag{8}$$

Since $H_{\mathrm{RRC}}(f)$ is only nonzero for $|f| \le \frac{1}{T}$, the effective integral range is restricted to $f \in [-\frac{1}{T}, \frac{1}{T}]$. Within the bandwidth of this range we assume that the shifted channel frequency response $H(f-\frac{\varepsilon-n}{T})$ is roughly a constant, *i.e.*, the channel coefficient on subcarrier n, denoted by H_n. As a result, (8) can be further formulated as

$$\begin{aligned} &\left(x(t)\cdot e^{j2\pi\frac{\varepsilon-n}{T}t}\right)\otimes\tilde{p}(t)\Big|_{t=l\cdot\frac{T}{2}} \\ &= H_n\sum_{n'=0}^{N-1}\sum_{l'=-\infty}^{+\infty} d_{n',l'}\theta_{n',l'}e^{j\pi l'(\varepsilon-n)}w(\varepsilon,\Delta n,\Delta l), \end{aligned}$$

where $\Delta n = n - n'$, $\Delta l = l - l'$, and $w(\varepsilon, \Delta n, \Delta l)$ as a function of the normalized CFO ε, subcarrier offset Δn and symbol offset Δl is defined as

$$w(\varepsilon,\Delta n,\Delta l) \triangleq \int_{-\infty}^{+\infty} e^{j\pi\Delta l T f}H_{\mathrm{RRC}}(f-\frac{\varepsilon-\Delta n}{T})H_{\mathrm{RRC}}(f)\mathrm{d}f.$$

Consequently, we have

$$R_1 = \sum_{n'=0}^{N-1}\sum_{l'=-\infty}^{+\infty} d_{n',l'}\Re\left\{H_n e^{j\tilde{\phi}(\varepsilon,n,l,n',l')}w(\varepsilon,\Delta n,\Delta l)\right\},$$

where $e^{j\tilde{\phi}(\varepsilon,n,l,n',l')} \triangleq e^{j\phi}e^{j\pi l'\varepsilon}e^{j\pi n\Delta l}e^{-j\frac{\pi}{2}(\Delta n+\Delta l)}$. Again we assume that with the help of pilot symbols, the phase of $H_n e^{j\tilde{\phi}(\varepsilon,n,l,n,l)}$ can be perfectly estimated and compensated, which results in

$$\begin{aligned} R_1 &= |H_n|\left(\sum_{n'=0}^{N-1}\sum_{l'=-\infty}^{+\infty} d_{n',l'}\alpha_n(\varepsilon,\Delta n,\Delta l)\right) \\ &= \Bigg[d_{n,l}\alpha_n(\varepsilon,0,0) + \sum_{\substack{l'=-\infty \\ l'\neq l}}^{+\infty} d_{n,l'}\alpha_n(\varepsilon,0,\Delta l) \\ &\quad + \sum_{\substack{n'=0 \\ n'\neq n}}^{N-1}\sum_{l'=-\infty}^{+\infty} d_{n',l'}\alpha_n(\varepsilon,\Delta n,\Delta l)\Bigg]\cdot|H_n|, \end{aligned} \tag{9}$$

where the definition

$$\alpha_n(\varepsilon,\Delta n,\Delta l) \triangleq \Re\left\{e^{-j\frac{\pi}{2}(\Delta n+\Delta l)}e^{j\pi\Delta l(n-\varepsilon)}w(\varepsilon,\Delta n,\Delta l)\right\}$$

applies. Note that $\alpha_n(\varepsilon, \Delta n, \Delta l)$ is the weight of each symbol to the detected symbol $\hat{d}_{n,l}$. In (9), the first summation term represents the desired signal, the second stands for the ISI on the detected subcarrier, and the last indicates the ICI plus ISI from all symbols on the other subcarriers. When signal power is concerned, the square of $\alpha_n(\varepsilon, \Delta n, \Delta l)$ should be taken and subscript n can be dropped since $|e^{j\pi\Delta l n}| = 1$.

It is assumed as before that the symbols on all subcarriers in the data sequence are independent from each other, and each has a power of $P_{\mathrm{S}}/2$, *i.e.*, the power of the original QAM symbols is P_{S}. The SINR at the detection of $d_{n,l}$ is given by

$$\mathrm{SINR}_{n,l}(\varepsilon) = \frac{\alpha^2(\varepsilon,0,0)}{\sum_{n'=0}^{N-1}\sum_{l'=-\infty}^{+\infty}\alpha^2(\varepsilon,\Delta n,\Delta l) - \alpha^2(\varepsilon,0,0) + \frac{\sigma^2}{|H_n|^2P_{\mathrm{S}}}}, \tag{10}$$

which follows from $\mathrm{E}\left[R_2^2\right] = \sigma^2/2$ as the real operation halves the noise power σ^2. Due to the assumed constant transmit power, the detected symbol index l in (10) can be set to 0 for simplicity. If the channel is flat fading, the subcarrier index n can be dropped as well.

Based on the above analysis, the effects of CFO on the desired signal include: its magnitude is scaled by $\alpha(\varepsilon, 0, 0)$; its phase is rotated by $\tilde{\phi}$ as defined earlier, which is to be compensated by the phase synchronizer; it is distorted by ICI and ISI, which only depend on the channel condition on the detected subcarrier.

4.1. ICI and ISI Analysis

When there is no CFO, the transmultiplexer under study with both ideal RRC filters at the transmitter and the receiver provides perfect reconstruction of the signal, *i.e.*,

$$\alpha(0, \Delta n, \Delta l) = \begin{cases} 1, & \Delta n = \Delta l = 0, \\ 0, & \text{otherwise.} \end{cases}$$

With a nonzero ε, the two immediately adjacent subcarriers and one of the secondly adjacent subcarriers, depending on the sign of ε, contribute to the interference. Due to the symmetry of the frequency response $H_{\mathrm{RRC}}(f)$, we discuss only the case that $\varepsilon > 0$ in the following.

The analytical expressions of the nonzero $w(\varepsilon, \Delta n, \Delta l)$ terms are given as follows:

$$\begin{aligned}
w(\varepsilon, 0, \Delta l) &= (1 - \tfrac{\varepsilon}{2}) e^{j\pi \Delta l \frac{\varepsilon}{2}} \left[\cos \pi \tfrac{\varepsilon}{2} \operatorname{sinc}\left(\Delta l (1 - \tfrac{\varepsilon}{2})\right)\right. \\
&+ \left. \frac{1}{2} \operatorname{sinc}\left((\Delta l + 1)(1 - \tfrac{\varepsilon}{2})\right) + \frac{1}{2} \operatorname{sinc}\left((\Delta l - 1)(1 - \tfrac{\varepsilon}{2})\right)\right], \\
w(\varepsilon, -1, \Delta l) &= \frac{1 - \varepsilon}{2} e^{j\pi \Delta l \frac{1+\varepsilon}{2}} \left[\cos \pi \frac{1 + \varepsilon}{2} \operatorname{sinc} \Delta l \frac{1 - \varepsilon}{2}\right. \\
&+ \left. \frac{1}{2} \operatorname{sinc}(\Delta l + 1) \frac{1 - \varepsilon}{2} + \frac{1}{2} \operatorname{sinc}(\Delta l - 1) \frac{1 - \varepsilon}{2}\right], \\
w(\varepsilon, 1, \Delta l) &= \frac{\varepsilon + 1}{2} e^{j\pi \Delta l \frac{\varepsilon - 1}{2}} \left[\cos \pi \frac{\varepsilon - 1}{2} \operatorname{sinc} \Delta l \frac{\varepsilon + 1}{2}\right. \\
&+ \left. \frac{1}{2} \operatorname{sinc}(\Delta l + 1) \frac{\varepsilon + 1}{2} + \frac{1}{2} \operatorname{sinc}(\Delta l - 1) \frac{\varepsilon + 1}{2}\right], \\
w(\varepsilon, 2, \Delta l) &= \frac{\varepsilon}{2} e^{j\pi \Delta l (\frac{\varepsilon}{2} - 1)} \left[\cos \pi \left(\frac{\varepsilon}{2} - 1\right) \operatorname{sinc} \Delta l \frac{\varepsilon}{2}\right. \\
&+ \left. \frac{1}{2} \operatorname{sinc}(\Delta l + 1) \frac{\varepsilon}{2} + \frac{1}{2} \operatorname{sinc}(\Delta l - 1) \frac{\varepsilon}{2}\right].
\end{aligned}$$

Analytical and numerical studies, *e.g.*, from Fig. 3 where the variations of α^2 over increasing symbol offset $|\Delta l|$ are demonstrated, show that

- $\alpha(\varepsilon, 0, 0) = w(\varepsilon, 0, 0) = (1 - \frac{\varepsilon}{2}) \cos \pi \frac{\varepsilon}{2} + \frac{\sin \pi \frac{\varepsilon}{2}}{\pi} < 1$;
- $\alpha(\varepsilon, \pm 1, 0) = 0$, *i.e.*, there is no pure ICI from the adjacent subcarriers;
- $\alpha(\varepsilon, \Delta n, \Delta l)$ converges to 0 when $|\Delta l| \to \infty$, yet the convergence of $\alpha(\varepsilon, \Delta n, \Delta l)$ is oscillatory due to the multiplication of sinc functions with a sinusoidal term;

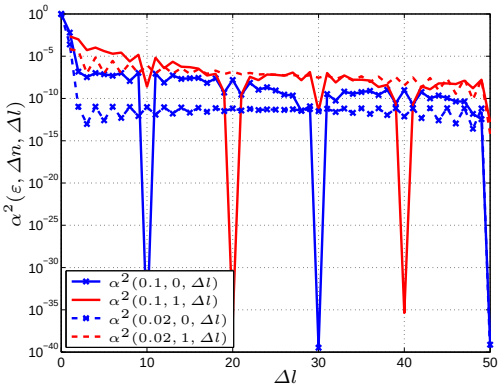

Fig. 3. Power attenuation factors

- $\alpha(\varepsilon, \Delta n, \pm 1)$, $\Delta n = 0, \pm 1$ contribute to the main part of interference.

4.2. Approximations With Very Small CFO

For $|\varepsilon| \ll \frac{1}{\pi}$, we neglect the terms $\alpha(\varepsilon, \Delta n, \Delta l), |\Delta l| > 1$ and apply the approximations $\sin(x) \approx x$, $\cos(x) \approx 1 - \frac{x^2}{2}$ and $\log_{10}(1 + x) \approx \frac{x}{\ln 10}$ to obtain an approximation of $D(\varepsilon)$ as

$$D(\varepsilon) \approx \frac{10}{\ln 10} \frac{3 \cdot \mathrm{SNR} + 4}{16} \pi^2 \varepsilon^2. \tag{11}$$

Compared with (5), it can be seen that the approximated SNR degradations are both proportional to the square of ε, and the degradation in FBMC systems is obviously smaller since the SNR in both approximations are linear and hence positive.

5. NUMERICAL RESULTS

In this section, the theoretically derived SNR degradations and their approximations in CP-OFDM and FBMC systems are numerically evaluated. Monte Carlo simulations are also done to verify these results. The number of subcarriers N is chosen to equal 1024, and for CP-OFDM system, the length of CP is set to $N/8$. Although in Sec. 3 and Sec. 4 the effects of CFO in multipath channels have been studied, we simulate here only with the AWGN channel to make a general comparison of the two systems, since it has been shown that the SNR degradation in the FBMC system only depends on the channel condition of the subcarrier of interest.

In Fig. 4, $D(\varepsilon)$ with ε up to 0.2 are shown, where the SNR is fixed to 0 dB. For the FBMC system, a slight gap between the theoretical and simulation curves can be read, which is due to the truncation of the RRC filter to the time interval $[-5T, 5T]$ in Monte Carlo simulations, which is shown to cause the system to be more sensitive against CFO as compared to FBMC systems with ideal RRC prototype filters. On the other hand, the approximations of $D(\varepsilon)$ as given by (5)

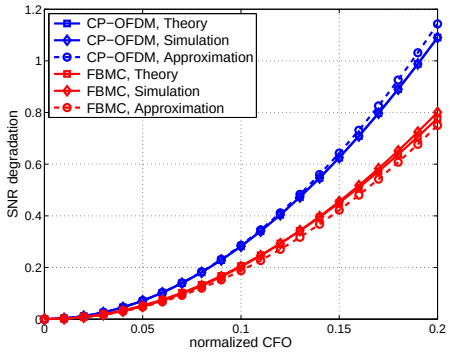

Fig. 4. SNR degradations vs. normalized CFO in CP-OFDM and FBMC systems with AWGN channel and SNR $= 0$ dB

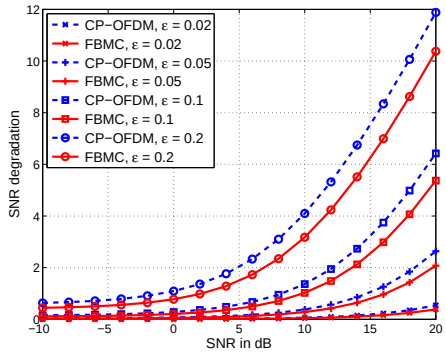

Fig. 5. SNR degradations vs. SNR in CP-OFDM and FBMC systems with AWGN channel and $\varepsilon = 0.02, 0.05, 0.1, 0.2$

and (11) also agree quite well with the theoretical results, especially when ε is small. Note that the approximation in FBMC system tends to be more optimistic as the ISI caused by symbols that are at least one symbol away from the one of interest is neglected.

Fig. 5 and Fig. 6 further illustrate with theoretical results the advantage of FBMC over CP-OFDM systems. In Fig. 5, the variations of SNR degradation with increasing receive SNR values are shown, which are roughly linear with very small CFO and the growth becomes slower than linear with larger CFO. In Fig. 6, the normalized CFO leading to fixed SNR degradations under various receive SNR are drawn, which demonstrates the more tolerance the FBMC systems have against CFO from another perspective, *e.g.*, if a loss of 1 dB in SNR is allowed, the CP-OFDM system can live with CFO's of up to 19% of the subcarrier spacing, whereas the FBMC system is able to live with a CFO of 23% of the subcarrier spacing.

6. CONCLUSIONS

In this paper, we have discussed and compared the effects of CFO on CP-OFDM and FBMC systems in multipath fading channels. Exact SNR degradation expressions as well as their approximations are reviewed for the CP-OFDM system and derived for the FBMC system. The advantage of FBMC systems as being less sensitive to CFO than CP-OFDM systems has been proved both by theory and simulations. The SNR degradations analyzed in this paper serve as an upper bound on real FBMC systems, since an ideal RRC prototype filter has been assumed which can not be implemented in practical systems. However, the analysis can help with CFO estimation and resource allocation in FBMC systems.

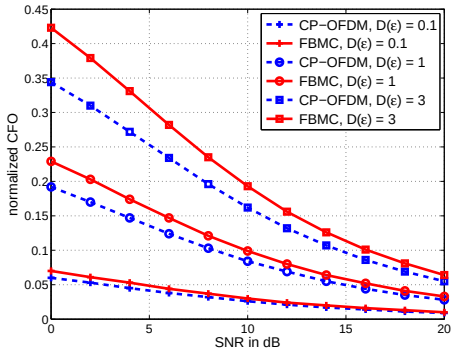

Fig. 6. Normalized CFO to cause SNR degradations of 0.1, 1 and 3 dB vs. SNR in CP-OFDM and FBMC systems with AWGN channel

7. REFERENCES

[1] Andrea Goldsmith, *Wireless Communications*, Cambridge University Press, 2005.

[2] T. Pollet and M. Moeneclaey, "The effect of carrier frequency offset on the performance of band limited single carrier and OFDM signals," *Global Telecommunications Conference*, vol. 1, pp. 719–723, November 1996.

[3] J. Lee, H. Lou, D. Toumpakaris, and J. M. Cioffi, "Effect of carrier frequency offset on OFDM systems for multipath fading channels," *IEEE Global Telecommunications Conference*, vol. 6, pp. 3721–3725, December 2004.

[4] Z. Zhang and C. Tellambura, "The effect of imperfect carrier frequency offset estimation on an OFDMA uplink," *IEEE Transactions on Communications*, vol. 57, pp. 1025–1030, April 2009.

[5] T. Fusco, A. Petrella, and M. Tanda, "Sensitivity of multiuser filter-bank multicarrier systems to synchronization errors," *ISCCSP 2008. 3rd International Symposium on*, pp. 393–398, March 2008.

[6] T. H. Stitz, A. Viholainen, T. Ihalainen, and M. Renfors, "CFO estimation and correction in a WiMAX-like FBMC system," *SPAWC'09. IEEE 10th Workshop on*, pp. 633–637, June 2009.